Vol. 189, No. 1, 1992 BIOCHEMICAL AND BIOPHYSICAL RESEARCH COMMUNICATIONS
November 30, 1992 Pages 488-495

ETHYLBENZENE HYDROXYLATION BY CYTOCHROME P450cam

D. Filipovic[a,c], M. D. Paulsen[b,c], P. J. Loida[a,d], S. G. Sligar[a,d,e], and R. L. Ornstein[b,e]

[a]Department of Biochemistry and Beckman Institute, University of Illinois, Urbana, Illinois 61801

[b]Molecular Science Research Center, Pacific Northwest Laboratory‡ Richland, Washington 99352

Received September 28, 1992

The metabolism of ethylbenzene by cytochrome P450cam was analyzed by experimental and theoretical methods. The present experiments indicate that ethylbenzene is hydroxylated almost exclusively at the secondary ethyl carbon with about a 2:1 ratio of R:S product. Several molecular dynamics trajectories were performed with different starting conformations of ethylbenzene in the active site of P450cam. The stereochemistry of hydroxylation predicted from the molecular dynamics simulations was found to be in good agreement with the observed products.

Cytochrome P450 are important enzymes in the synthesis of steroids, fatty acids, and prostaglandines, as well as the metabolism of xenobiotics. The superfamily of cytochromes P450 metabolizes a plethora of substrates ranging from ethylene to cyclosporine A, with an amazing variety of chemical reactions including hydroxylation of carbon and heteroatoms, dealkylation of amines and ethers, epoxidation of double bonds, and reductive dehalogenation (for a review see 1). Common to most of these reactions is

[c]Supported by the Northwest College and University Association for Science in affiliation with Washington State University under Contract DE-AMO6-76-RLO 2225 with the U. S. Department of Energy, Office of Energy Research.

[d]Supported in part by the Biological Research and Development Corporation and NIH grant GM31756.

[e]To whom correspondence should be sent.

‡Pacific Northwest Laboratory is operated for the U. S. Department of Energy by Battelle Memorial Institute under Contract DE-ACO6-76RLO 1830.

0006-291X/92 $4.00

the formation of a still hypothetical, iron-oxo intermediate. The type of reaction being performed depends only upon the nature and mobility of the substrate (for a review see 2). The understanding, prediction, and control of P450-substrate interactions is therefore of paramount interest for engineering cytochromes P450 as biotechnological tools or design of therapeutical inhibitors.

Cytochrome P450cam catalyzes the regio- and stereospecific hydroxylation of camphor initiating the complete degradation of this monoterpene, allowing the soil bacterium *Pseudononas putida* to utilize camphor as a sole carbon source for the organism. High resolution crystal structures are available for P450cam with a variety of substrates and inhibitors (for a review see 3). This strong structural library allows one to investigate the functional roles of active site residues with a combination of site-directed mutagenesis techniques (for a review see 4), functional characterization, as well as theoretical 5, 6) and recent molecular dynamics studies (7-11). Thus, site-directed mutagenesis in concert with high resolution crystal structures and computational methods now offers the possibility to change P450cam properties on a rational basis (12). In the present study, we have used ethylbenzene as a model system to investigate the binding and metabolism of small substrates by cytochrome P450cam. Ethylbenzene offers the possibility to study several aspects of P450 catalysis and protein-substrate interactions such as the influence of different carbon reactivities on the product profile, stereochemistry of hydroxylation at the secondary carbon center (13), and substrate camphor. We report a comparison between the computationally derived and experimentally observed product profiles of ethylbenzene hydroxylation by wild-type P450cam.

Model and Methods

Model

The x-ray structure of the phenimidazole-cytochrome P450cam complex (14), kindly provided by T. M. Poulos, served as the starting point of our model of ethylbenzene-bound cytochrome P450. Three starting conformations were used for the substrate. The first starting structure was modeled by superimposing the phenyl ring of ethylbenzene onto the phenyl ring of 4-phenimidazole from the inhibitor-P450cam complex (14). This conformation places the pro-S hydrogen in a favorable abstraction geometry. In the second conformation ethylbenzene was docked to favor R-hydroxylation. These two orientations are shown in Figure 1. The third starting structure, used as a control (see below) was a random snapshot from one of the previous trajectories. Because we were interested in modeling the hydrogen abstraction step as closely as possible, we included an iron-bound activated oxygen atom in our simulation.

An all hydrogen model was used and the polar sidechain hydrogens were added as described previously so as to maximize hydrogen bonding (15). With the exception of the heme group, the standard Discover (Biosym Technologies) forcefield was used (16). The heme parameters were similar to those used previously in simulations of camphor-bound cytochrome P450cam (10). New parameters were determined for the iron-oxo intermediate and are listed in Table 1. The charges and forcefield parameters for ethylbenzene were taken from the standard Discover library.

Theoretical Methods

The starting structures were first minimized in a four step process. The added hydrogen atoms were relaxed with all heavy atom positions fixed. Then the

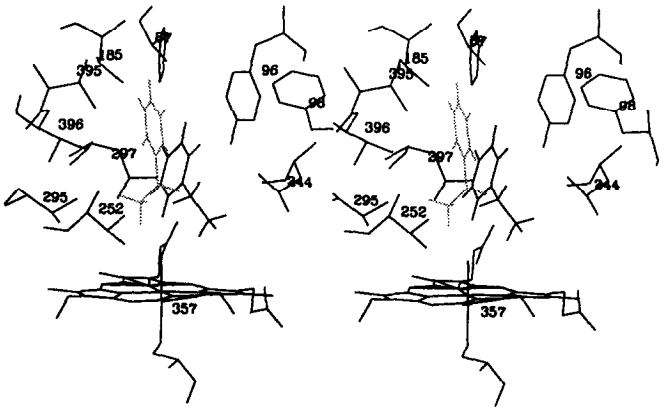

Figure 1. The two views of the P450cam active site are the minimized starting structures for the different molecular dynamics trajecatories.

cystallographic waters and the docked substrate were relaxed while holding the protein fixed. Finally, the energy of the entire system was minimixed with 500 steps each of steepest descents and conjugate gradients minimization. For each MD trajectory, initial velocities were randomly assigned from a Boltzmann distribution at 50 K. The system was then slowly warmed to 300 K for 10 psec after which the velocities were reinitialized at 300 K and the trajectories were continued for an additional 30 psec. Structures were saved every 0.25 psec.

Table 1. Forcefield Parameters for the Iron-Oxo Complex

Partial Atomic Charges in Ferryl Intermediate

Atom	Charge
Fe	1.28
S	-0.10
O	-0.50

Nonbonded Parameters for Ferryl Intermediate

Atom	A (Kcal/A^{12})	B (Kcal/A^6)
S	365906.4	250.8
O	272894.78	498.88
Fe	3355443.0	1638.4

Bond Parameters for Ferryl Intermediate

bond	re (A)	K (kcal/mole)
Fe-S	2.20	120.0
Fe-O	1.78	300.0

Angle Parameters for Ferryl Intermediate

angle	theta (degrees)	K (cal/degree)
N-Fe-O	90.0	50.0
S-Fe-O	180.0	10.0

Experimental Methods

Cytochrome P450cam, putidaredoxin and putidaredoxin reductase were overexpressed in *E. coli* and purified as previously described (17, 18). Typical incubations (20 min at 25°C) contained 0.5 μM P450cam, 5 μM putidaredoxin reductase, 10 μM putidaredoxin, 1nM ethylbenzene, 200 mM potassium chloride, and 500 μM NADH in a total volume 1 ml 50 mM Tris, pH 7.4 Products were isolated by extraction of the total reaction with two volumes of $CHCl_3$ and subjected to gas chromatographic analysis on a 0.25 mm x 15 m DB-1 capillary column (J & W Scientific). The *sec*-phenethylalcohols were separated on a 0.25 mm x 30 m Cyclodex B capillary column (J & W Scientific) programmed to run at 110°C for 20 mins, then to rise at 1 deg. min to 130°C. The retention times for the R-*sec*, and S-*sec* phenethylalcohol enantiomers were 32.9 and 34.1 min, respectively. Individual peaks were identified using the commercially available phenethyl alchohols as standards (Aldrich). Product yields were determined by addition of a known amount of an internal standard prior to extraction and correcting peak areas of products to account for any deviation from the theoretical peak areas of the internal standard, assuming 100% recovery.

Results and Discussion

Five MD simulations were run for the three different starting orientations of ethylbenzene for 40 psec each. The resulting 805 structures (coordinates were saved every 0.25 psec) were analyzed to determine the relative orientation of the C7 and C8 carbons and their respective hydrogens to the ferryl oxygen. The hydrogens of the terminal, tertiary carbon of ethylbenzene were found to have more active conformations than those of the secondary carbon (Figure 2a), but only the latter were further analyzed, since a secondary radical is known to be much more stable than a tertiary one (5, 7, 13). This same phenomenon is observed in camphor-bound P450 where the tertiary C9 carbon is also in a favorable hydrogen abstraction position roughly 50% of the time but only the methylene C5 carbon is hydroxylated (Figure 2b). For the prediction of stereospecificity only snapshots with the hydrogens closer than 3.5 Å and an oxygen-hydrogen-carbon angle of 180±45° were counted. Other conformations were considered to be nonreactive for hydrogen abstraction. The cutoff was chosen based on simulations with several substrates where it was found that these criteria gave the expected regio-specificity in agreement with experimental observations (9, 19). This analysis predicts a product ratio (R/S) of 76/24 based solely on the probability of pro-S and pro-R abstraction, respectively.

We were also interested in determining whether or not the trajectory could be used to predict the coupling between product formation and NADH consumption. In the case of a camphor-bound trajectory, virtually all of the structures examined were active conformations based on the above discussed cutoff criteria. This is consistent with the high degree of coupling observed experimentally for camphor hydroxylation. Analysis of the ethylbenzene trajectories revealed 42 active conformations out of 805 total structures, thus resulting in the prediction of 5.2% coupling of product formation and NADH consumption based on a combination distance and angle criteria.

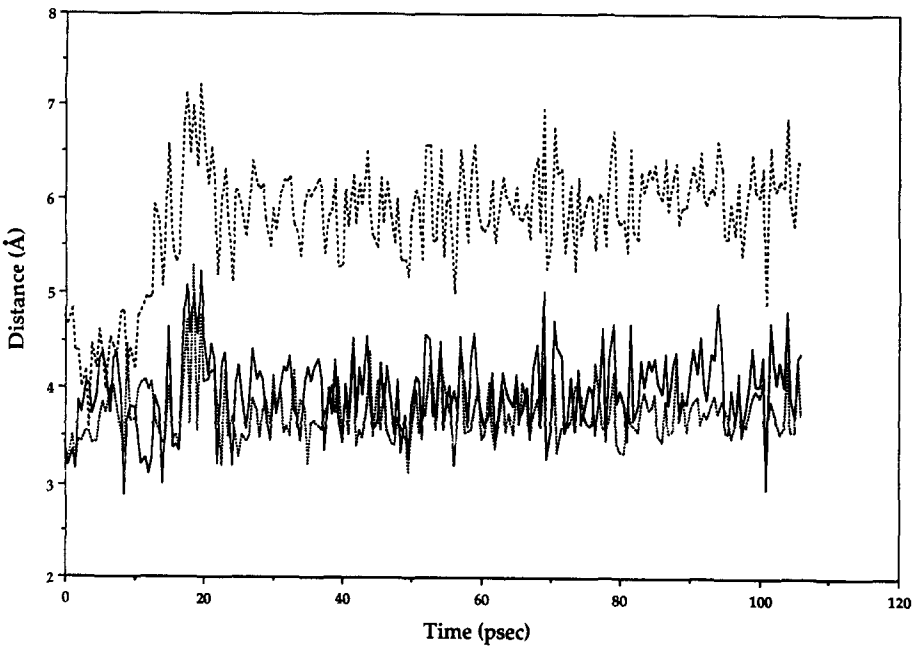

Figure 2 a. Distance between C7, C8, and the center of mass of ethylbenzene and the ferryl oxygen atom as a function of the timecourse of the simulation. The solid, dotted and dashed curves monitor the distances involving C7, C8, and the center of mass, respectively.

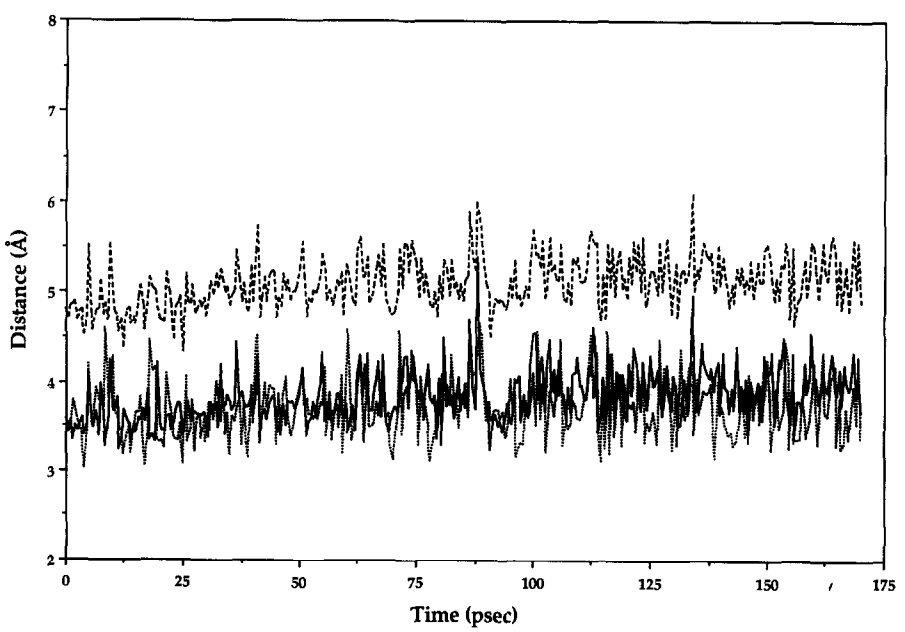

Figure 2b. Distance between C5, C9, and the center of mass of camphor and the ferryl oxygen atom as a function of the timecourse of the simulation. The solid, dotted and dashed curves monitor the distances involving C5, C9, and the center of mass, respectively.

In simulations of camphor analogs the effect of initial velocities on the predicted specificity is small (19) in part because the most probable substrate orientation has been experimentally determined and the complementarity between the substrate and the active site is better. For valproic acid and methyl styrene, however (7, 20), where no experimental information about the starting conformation is available, the predicted specificity varies substantially between different simulations. A similar difficulty was noted also in this study. We observed significant variations of the predicted R/S ratio and coupling in the four initially performed 40 psec trajectories. Therefore, one additional simulation was performed in order to check the stability of the calculation and determine the influence of one additional run on the convergence of the results. The addition of this trajectory with a different starting orientation I in the analysis altered the predicted R/S ratio by only a modest amount (6%) and changed the predicted coupling by less than 1%. This suggests that even for compounds which are not close analogs of the native substrate convergence in the calculated product specificity can be achieved with sufficient sampling.

In order to address the question whether it is more suitable to run one long trajectory or perform several short runs with different starting conformations and/or initial velocities, we extended one of the simulations to 110 psecs (Figure 2a). The fact that no major reorientations were observed in the 40-110 psec region suggests that multiple shorter runs might better sample the available configuration space. This will be particularly important for substrates with low complementarity to the heme pocket and when no structural information is available.

The experimentally-obtained products were analyzed first by conventional GC. Ethylbenzene is processed by P450cam to 98% at the benzylic position affording the *sec*-phenethylalcohol. Only traces of 2-phenylethanol or of ethylphenols were found. These results are in agreement with a study of White and coworkers (13), who also observed only the benzylic alcohol as a product of ethylbenzene hydroxylation by the mammalian isozyme P450LM2. Separation of the *sec*-phenthylalcohol enantiomers was accomplished using a chiral capillary GC column. Analysis of the product mixture shows that it consists of 73% R and 27% S sec-phenethylalcohol, which is in reasonable agreement with the molecular dynamics prediction of a 76:24 ratio. It has to be emphasized that it could not be expected that this small substrate would be hydroxylated with high stereospecificity, since it lacks polar functions to form a hydrogen bond with tyrosine 96 and it is too small to be contoured and positioned by the heme pocket.

White and coworkers (13) investigated the hydroxylation of ethylbenzene by P450LM2 with a series of deuterated substrates and observed a considerable loss of stereochemistry between the hydrogen abstraction and hydroxy recombination steps. The good agreement between the experimental values and the probabilities for pro-R and pro-S abstraction in our study does not indicate such a crossover event with P450cam, although only a detailed study using labeled ethylbenzenes can completely clarify this point.

In addition to determining the product stereochemistry, the coupling between product formation and NADH consumption was determined. The low (6%) coupling is in good agreement with the theoretically determined value (5.2%) and indicates water access to the active site. This finding is not surprising, since ethylbenzene is a significantly smaller substrate than camphor and it is knows that small substrates are unable to expel active site waters completely (21). The other explanation, that low coupling is due to a high mobility of ethylbenzene, is less favorable, since as seen in Figure 2a and the distance from the ferryl oxygen to the center of mass of ethylbenzene is fluctuating only slightly more than for camphor which is highly immobilized in the active site. Accurate guesses about the expected coupling of a P450 reaction will be of some importance for predicting whether a naturally occurring or designed isozyme will be suitable for a biotechnological application not only because reducing equivalents are costly, but especially since uncoupling is usually related to autooxidation pathways and peroxide formation (22, 23), jeopardizing enzyme activity.

To our knowledge, this is the second investigation where the metabolism of small substrates by P450cam was examined both, by experimental and theoretical methods. As in the report by Ortiz de Monetellano et al. (11), a remarkable agreement between the computational and biochemical results was found. This result is particularly interesting, since another substrate as well as a different method of simulation and analysis was used. Moreover, we successfully used computational methods to examine the coupling of the reaction. Our work, therefore, conforms and further expands the general validity of computational methods in characterizing and predicting the binding and metabolism of small substrates to P450cam. The insight gained with work on P450cam will also help guide future work on membrane bound P450 isozymes as soon as reliable models of a membrane bound P450 become available.

References

(1) Porter, T.D., Coon, M.J., J. Biol. Chem. 266, 13469 (1991)
(2) Guengerich, P. F., J. Biol. Chem. 266, 12167 (1991)
(3) Poulos, T. M., Meth. Enzymol. 205, in press (1991)
(4) Sligar, S. G., Filipovic, D., Stayton, P. S., Meth. Enzymol. 206, in press (1991)
(5) Collins, J. R., Loew, G. H., J. Biol. Chem. 263, 3164 (1988).
(6) Luke, B. T., Collins, J. R., Loew, G. H., McLean, A. D., J. Am. Chem. Soc. 112, 8686 (1991)
(7) Collins, J. R., Camper, D. L., Loew, G. J., J. Am. Chem. Soc. 113, 2736 (1991)
(8) Paulsen, M. D., Ornstein, R. L., Proteins 11, in press (1991).
(9) Paulsen, M. D., Bass, M. B., Ornstein, R. L., Biomol. Struc. and Dyn. 9, in press (1991)
(10) Bass, M. B., Paulsen, M. D., Ornstein, R. L., Proteins: Struc., Funct., Genet., in press (1991)
(11) Ortiz de Montellano, P. R., Fruetel, J. A., Collins, J. R., Camper, D. L., Loew, G. H., J. Am. Chem. Soc. 113, 3195 (1991)
(12) Bass, M. B., Filipovic, D., Sligar, S. G., Ornstein, R. L., Prot. Eng. submitted (1992)
(13) White, R. E., Miller, J. P., Favreau, L. V., Bhattachaaryya, A. J., J. Am. Chem. Soc. 108, 6024 (1986)

(14) Poulos, T. M., Howard, A. J., Biochemistry 26, 8165 (1987)
(15) Bass, M. B., Hopkins, D. F., Jaquysh, W. A. N., Ornstein, R. L., Proteins, in press (1991)
(16) Dauber-Osguthorpe, P., Roberts, V. A., Osguthorpe, D. J., Wolff, J., Genest, M., Hagler, A. T., Proteins 4, 31 (1988)
(17) Stayton, P. S., Sligar, S. G., Biochemistry 30, 1845 (1991)
(18) Davies, M. D., Quin, L., Beck, J. L., Suslick, K. S., Koga, H. J., Horiuchi, T., Sligar, S. G., J. Am. Chem. Soc. 112, 7396 (1990)
(19) Paulsen, M. D., Ornstein, R. L., in preparation
(20) Loew, G. H., Collins, J. R., Int. J. Quant. Chem., in press
(21) Fisher, M. T., Sligar, S. G., J. Am. Chem. Soc. 107, 5018 (1985)
(22) Gorsky, L. D., Kopp, D. R., Coon, M. J., J. Biol. Chem. 259, 6812 (1984)
(23) Atkins, W. M., Sligar, S. G., J. Am. Chem. Soc., 109, 3754 (1987)